



# Effect of salt valency and concentration on shear and extensional rheology of aqueous polyelectrolyte solutions for enhanced oil recovery

Anna V. Walter<sup>1</sup> · Leidy N. Jimenez<sup>2</sup> · Jelena Dinic<sup>2</sup> · Vivek Sharma<sup>2</sup> · Kendra A. Erk<sup>1</sup>

Received: 9 May 2018 / Revised: 17 January 2019 / Accepted: 21 January 2019 / Published online: 12 February 2019  
© Springer-Verlag GmbH Germany, part of Springer Nature 2019

## Abstract

The injection of polymer solutions into an oil basin can lead to enhanced oil recovery (EOR) by increasing the microscopic sweep of the reservoir, improving the water-oil motility ratio, and thus leading to greater yield from oil fields. In this contribution, we characterize both shear and extensional rheological response of aqueous solutions of partially hydrolyzed polyacrylamide (HPAM), the most commonly used polymer for EOR, for velocity gradients in both the flow direction (extensional) and perpendicular to flow (shear) arise in EOR applications. As HPAM is a charged polymer, to better emulate the environment in oil basins, the rheological response was investigated in presence of salt, sodium chloride, and calcium chloride, with concentrations  $3.7 \times 10^{-4}$ –1.5 M, as a function of polymer molecular weight (2–10 million g/mol) and concentration (0.005–0.3 wt%). The extensional relaxation times and extensional viscosity are measured using dripping-onto-substrate (DoS) rheometry protocols, and a commercial shear rheometer was utilized for characterizing the shear rheology response. The polyelectrolyte solutions formed by HPAM exhibit shear thinning in steady shear, but show strain hardening in response to extensional flow. Even though an increase in monovalent salt concentration leads to a decrease in both shear viscosity and extensional relaxation times, an increase in divalent salt concentration leads to an increase in extensional viscosity and relaxation time, implying that ion coordination can play a role in the presence of multivalent ions.

**Keywords** Polyelectrolyte · Rheology · Extensional flow · Salt condensation

## Introduction

Energy generated from fossil fuels makes up the majority of global energy production and consumption, with over 32% of the world's primary energy consumption derived from oil ("BP Statistical Review of World Energy June 2014," 2014). However, at the current rate of production and consumption, the world's current known oil will last only 54 years. Most oil reservoirs produce only 20–40% of the oil originally in place (OOIP) (Advanced

Resources International 2006; Olajire 2014); accessing the remaining oil could greatly increase the time for which oil is available. Enhanced oil recovery (EOR) seeks to reach this oil and has shown to allow up to 65% of the OOIP to be recovered (Advanced Resources International 2006). Traditionally, oil recovery starts by utilizing the pressure differential between the surface and the oil basin. During waterflood, also known as secondary recovery, water is injected into the basin to recreate this pressure differential. Enhanced oil recovery, or tertiary recovery, goes beyond the use of water. There are many methods of EOR, including water-alternating-gas, in which a waterflood and a gas flood are alternated, and chemical flooding in which chemicals are added to the waterflood. One type of chemical EOR, alkaline-surfactant-polymer (ASP) flooding, has enabled recovery of 83% of the OOIP (Shutang et al. 1995). In ASP EOR, alkali and surfactant are added to the waterflood; a separate waterflood containing polymer often follows (Muggeridge et al. 2014). This polymer in the waterflood causes the viscosity of the water phase to increase. This improves recovery of oil by increasing

**Electronic supplementary material** The online version of this article (<https://doi.org/10.1007/s00397-019-01130-6>) contains supplementary material, which is available to authorized users.

✉ Kendra A. Erk  
erk@purdue.edu

<sup>1</sup> School of Materials Engineering, Purdue University, 701 West Stadium Avenue, West Lafayette, IN 47907, USA

<sup>2</sup> Department of Chemical Engineering, University of Illinois at Chicago, 810 S. Clinton St, Chicago, IL 60607, USA

the capillary number and decreasing the mobility ratio between oil and water, improving the microscopic and macroscopic sweep efficiency, respectively (Muggeridge et al. 2014; Olajire 2014).

Partially hydrolyzed polyacrylamide (HPAM) is a polymer commonly used in EOR for its high viscosity in solution (Wever et al. 2011). The structure of HPAM is shown in Fig. 1. In solutions with pH above the pKa of polyacrylic acid (between 6 and 7) (Katchalsky and Spitnik 1947; Petrov et al. 2003), the polyacrylic acid repeat units are deprotonated and adopt a negative charge. In the aqueous solutions of HPAM that incorporate sodium acrylate rather than acrylic acid in the repeat unit, the chain adopts a negative charge and the sodium ions form a diffuse layer close to the chain, approximately within a distance (Debye length) determined by ionic strength. The percent hydrolysis of HPAM represents the portion of repeat units that are hydrolyzed to form acrylic acid or sodium acrylate. Thus, percent hydrolysis acts as a measure of the charge fraction or the relative number of charges on the polymer backbone. See Eq. 1, where  $m$  is the number of hydrolyzed monomers and  $n + m$  is the total degree of polymerization (Lewandowska 2006).

$$\% \text{hydrolysis} = \frac{m}{n + m} * 100\% \quad (1)$$

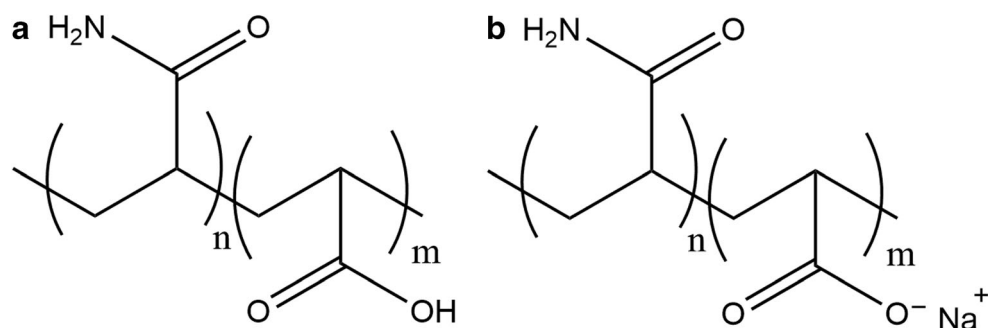
In oil basins, HPAM is often in the deprotonated state (Muggeridge et al. 2014), and as the charged groups repel each other in solution, the polymers adopt an expanded conformation. Polymers like HPAM that have charge bearing monomers in their repeat unit are known as polyelectrolytes. Aqueous polyelectrolyte solutions are used in a variety of technical applications, including drinking water filtration (Weidman et al. 2016) and treatment (Metaxas et al. 2018), additives for cementitious materials (Murray and Erk 2014), and as rheology modifiers for formulations used in pharmaceutical, food, cosmetics, paints, and coatings industries (Radeva 2001; Calvert 2001). In salt-free solutions, the electrostatic expansion caused by the charges along the polymer results in a relatively low overlap concentration ( $c^*$ ) for polyelectrolytes in comparison with  $c^*$  for neutral polymers (Colby 2010). Solutions with polymer concentration below the

overlap concentration are considered to be in the dilute regime, and above the overlap concentration are said to be in the semi-dilute regime (Colby 2010). Experimentally, the overlap concentration can be identified as the concentration at which solution viscosity becomes twice the solvent viscosity (Colby 2010).

In dilute solutions without other ions present, polyelectrolytes adopt an extended conformation due to the electrostatics-induced charge repulsion, and show  $R \sim N$ , where  $R$  is the radius of gyration and  $N$  is the number of repeat units or ideal blobs. This is in contrast to  $R \sim N^{1/2}$  (for theta solvents) observed for neutral polymers (Colby 2010; De Gennes et al. 1976). The larger coil sizes for polyelectrolytes in solution make accessing the dilute regime experimentally challenging as the overlap concentration is quite low (Rubenstein and Colby 2003). The coil size changes dramatically above the overlap concentration in the semi-dilute regime, where inter-chain interactions, together with the role played by long and short-range electrostatic interactions, impact the conformations and the rheological response (Colby 2010; Schweins and Huber 2001; Volk et al. 2004). However, at present, polymer entanglements in aqueous salt solutions are not well-understood, though unlike neutral solutions, the unentangled semi-dilute regime usually spans more than one decade in concentration. Scaling laws seem to capture the concentration-dependent variation in shear rheological response of charged polymers in the low or no salt added limit (Colby 2010). The effect of added salt, especially multivalent salt, on the rheological properties of polyelectrolytes is less well understood and is the focus of this study.

In particular, even though electrostatic interactions are known to play a critical role in determining polyelectrolyte conformation and rheological response for HPAM in oil fields of varying salinity, a priori determination of such effects can be quite challenging since the valency, type and concentration of counterions may vary geographically (Muggeridge et al. 2014; Rashidi et al. 2010). Water is generally present in an oil basin at formation and this connate water has a variety of salts present (Timm and Maricelli 1952). In the Illinois basin, USA, the most prevalent monovalent cation is  $\text{Na}^+$  and the most prevalent divalent cation is  $\text{Ca}^{2+}$ , whereas chloride ( $\text{Cl}^-$ ) is the most common anion (Stueber and Walter 1991; Stueber

**Fig. 1** Chemical structure of HPAM. (a) the polyacrylic acid form and (b) the sodium salt, sodium acrylate. The degree of hydrolysis is given in Eq. 1. When dissolved in solutions with  $\text{pH} > 7$ , the carboxylic acid groups shown in (a) deprotonate, creating a negative charge along the polymer backbone



et al. 1993). Monovalent cations such as  $\text{Na}^+$  often act in solution to screen charges on polyelectrolytes from one another, thus reducing the electrostatics induced stretching and consequently also the radius of the polymer coils in solution (Volk et al. 2004). This in turn alters the overlap concentration of the solution, and also influences both the intrachain and interchain interactions, which in turn influences the rheological behavior of the solutions.

While the presence of monovalent salts generally decreases the polymer coil size, divalent charges can interact with polyelectrolytes in a multitude of ways. The divalent cations can form specific ion pairs with the negative charges either along a polymer backbone (intrachain pairs) (Huh et al. 2009) or between charges on different polymer chains (interchain). The divalent cations can associate with the polyanion chains by undergoing “manning condensation” in which the cations are closely associated with the chain so as to keep the local charge density electrically neutral (Schweins and Huber 2001). These effects can cause the polymer chain to collapse into a tight coil or even a “pearl necklace” conformation, consisting of collapsed chain segments connected together (Schweins and Huber 2001). Many studies have investigated the effect of sodium (Jung et al. 2013; Sedaghat et al. 2013; Ward and Martin 1981; Odell and Haward 2008) or calcium (Francois et al. 1997; Huh et al. 2009; Sheng 2011; Ward and Martin 1981; Odell and Haward 2008) cations on the conformation and behavior of HPAM and other water-soluble polymers in aqueous solutions. The literature however is inconclusive on the conformation of HPAM in the presence of aqueous divalent calcium. It is generally observed that when calcium and sodium cations are both present in solution with HPAM, the solution shear viscosity is lower than that with only sodium present (Huh et al. 2009; Ward and Martin 1981). The mechanism of interaction between divalent ions and polyelectrolytes in solution (both with or without additional monovalent ions) is still under debate. Some papers suggest intermolecular interactions, or two distinct polymer chains bridged by a calcium ion. Others suggest intramolecular interactions (Odell and Haward 2008) or a transition between inter- and intramolecular interactions (Francois et al. 1997).

Here, we investigate the nature and influence of interactions between commercial HPAM and salt ions in aqueous solutions via shear and extensional rheometry. Rheological response is exquisitely sensitive to polymer conformations and degree of overlap, i.e., to the influence of both intrachain and interchain interactions. In this study, type (valency) and concentration of salt in aqueous solutions are varied as well as a range of polymer molecular weights and concentrations. The range of shear rates tested mimic the range of shear rates experienced during both the pumping of solutions and the shear rates encountered in the oil basin. Though shear rheology of polyelectrolyte solutions (especially in presence of monovalent counterions) has been the focus of many studies

(Boris and Colby 1998; Colby 2010; Jung et al. 2013; Sedaghat et al. 2013), there are only a few reported measurements of the extensional rheology response (Dunlap et al. 1987; Jimenez et al. 2018; Miles et al. 1983; Rodríguez-Rivero et al. 2014). In porous media, the flow field is extensional in nature as the fluid traverses through converging and diverging channels. In the current contribution, we characterize the extensional rheology response of polyelectrolyte solutions using the dripping-onto-substrate extensional (DoS) rheology technique (Dinic et al. 2017a; Dinic et al. 2017b; Dinic et al. 2015; Jimenez et al. 2018). The DoS rheometry relies on quantifying both extensional viscosity and extensional relaxation time by analysis of capillary-driven thinning and pinch-off dynamics of an unstable fluid neck formed by dripping a finite volume of fluid from a nozzle onto a substrate. Therefore, combined with shear rheometry, DoS rheometry allows us to model the complete rheological profile of polyelectrolyte solutions for EOR while investigating the effect of counterion type and concentration on rheological behavior.

## Materials and methods

Commercial polymers made by SNF (Andrézieux, France) in their FLOPAAM series were used in this study without further purification. The reported molecular weight and approximate degree of hydrolysis for three commercial polymers used are shown in Table 1 (Seright et al. 2011; SNF n.d.; Veerabhadrapa et al. 2013). Solid sodium chloride,  $\text{NaCl}$ , and anhydrous calcium chloride,  $\text{CaCl}_2$ , were used as received to modify the salinity of solutions.

Solutions for shear and extensional rheology were prepared by mixing an appropriate amount of polymer and salt, followed by overnight stirring using a magnetic stir bar, and sonication for 1 h in a bath sonicator. Solutions at very low polymer concentrations were prepared by serial dilution. For shear rheometry, solutions contained 0.30 wt% of FLOPAAM 3330; the concentration of  $\text{NaCl}$  ranged from  $3.7 \times 10^{-4} \text{ M}$ –1.5 M and the concentration of  $\text{CaCl}_2$  ranged from 0.0386 M–1 M. These salt concentration ranges were chosen to approximate the range of monovalent and divalent ion concentrations found in oil basins (Pan 2005; Stoll et al. 2011; Timm and Maricelli 1952). Solutions that were used for

**Table 1** Physical properties of FLOPAAM samples used in this study

FLOPAAM species	Reported molecular weight	Approximate % hydrolysis
3330 s	8–10 million g/mol	25–30
3230 s	4–6 million g/mol	25–30
3130 s	1–2 million g/mol	25–30

extensional rheometry span a wide range of concentrations so that the semi-dilute and dilute regimes of polymer solutions may be accessed. Solutions of FLOPAAM 3130, 3230, and 3330 were used at 0.005, 0.025, 0.05, 0.1, and 0.3 wt% of polymer. Salt concentrations were either 0.0386 M or 1 M for each salt, chosen to model basins with relatively high and low salinity. There was no visual evidence of precipitation or coacervation, and the solutions remain colorless and transparent over the course of the investigation. Solutions were investigated within a week of preparation, as preliminary data indicated that solution behavior over the shear rate range of interest was unchanged during this time.

## Shear rheometry

The Anton Paar MCR 702 was used in single drive mode for all shear rheometry experiments. All shear rheometry measurements were performed with the double gap fixture with diameter of 26.7 mm (DG26.7) at a constant temperature of 25 °C, maintained by a Peltier heating system with water as the heat transfer fluid.

The shear rheology experiments were carried out on a torsional rheometer using the experimental protocol outlined in Fig. 2. A constant shear rate of 1 s<sup>-1</sup> was applied for 10 min, with measurements being recorded every 6 s for a total of 100 measurements. The shear rate was then ramped logarithmically from 1 s<sup>-1</sup> to 10 s<sup>-1</sup> with 5 points per decade and 30 s allowed per point. A shear rate of 10 s<sup>-1</sup> was then applied and maintained for 10 min, again with measurements taken every 6 s. This process was repeated for 100 s<sup>-1</sup> and 500 s<sup>-1</sup>. After the measurement at a constant 500 s<sup>-1</sup>, the shear rate was ramped from 500 s<sup>-1</sup> to 1 s<sup>-1</sup>. The focus of the measurements was the assessment of steady shear viscosity values at the shear rates experienced by solutions during EOR

applications. Solutions in EOR applications typically experience high shear rates (500 s<sup>-1</sup> or more) during pumping, but lower shear rates (1 s<sup>-1</sup> or less) in transit and in the oil basin. This procedure was repeated with 5 aliquots of the same solution.

Viscosity measurements reported here are the average of the measurements taken from the last 200 s during constant shear. The outlined procedure ensures that the viscosity values reported here are extracted from the steady shear, and in experiments reported here, the last 200 s of data is generally stable, as seen in Fig. 2b. The measurements conducted by ramping the shear rate up were contrasted with measurements made using ramp down to assess both the possibility of aggregate formation and hysteresis.

## Extensional rheometry

Extensional viscosity and extensional relaxation time were measured using the dripping-onto-substrate (DoS) rheometry (Dinic et al. 2017b; Dinic et al. 2015) set-up shown schematically in Fig. 3. A finite volume of polyelectrolyte solution is released from the nozzle onto a substrate using a syringe pump at a relatively low flow rate of  $Q = 0.02$  ml/min (kept constant in all experiments). The syringe pump is switched off just as the drop touches the substrate, and even before the liquid neck emerges. The shape and shape evolution of the liquid neck formed between a sessile drop and the nozzle undergoes self-thinning that is completely determined by the local balance of forces, and retains no memory or influence of the flow history (Dinic et al. 2015; Dinic et al. 2017b). The distance between the nozzle and substrate  $H$  is kept constant, and experiments described here were carried out for an aspect ratio  $H/R_0 = 3$ , where  $R_0$  is the radius of the nozzle. The stretched capillary bridge formed between the nozzle and the sessile drop is visualized

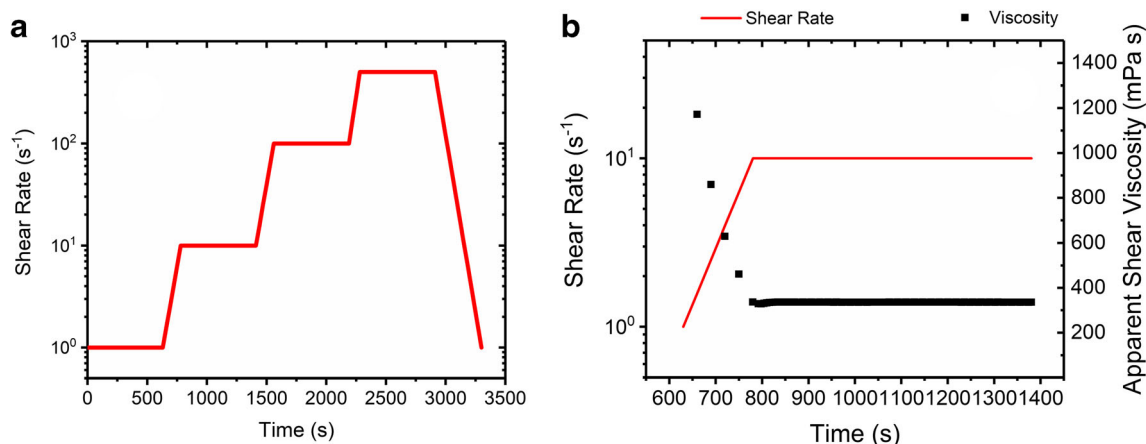
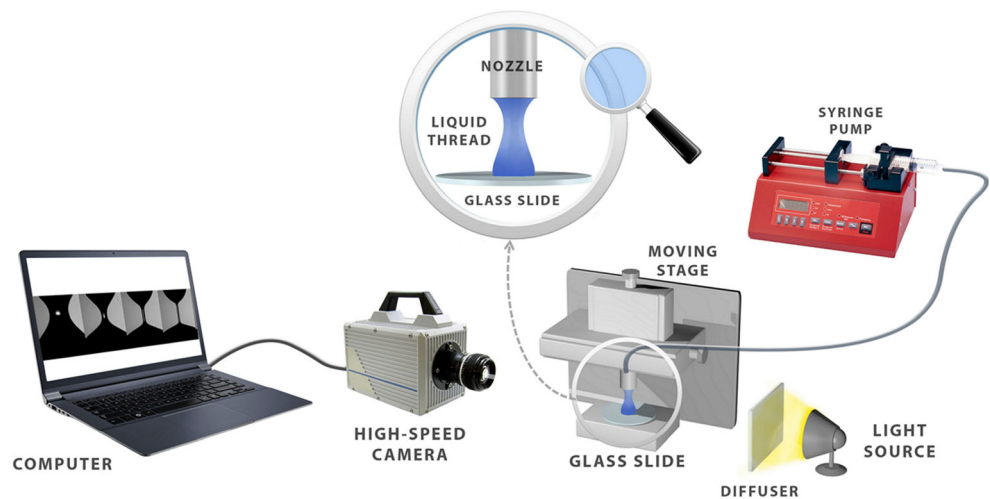


**Fig. 2** (a) Shear rate applied during all shear rheometry tests. For each sample, this procedure was repeated for a total of five times, using a new aliquot each time. (b) An example of applied shear rate (solid line) and

measured viscosity (points) during one plateau. Viscosity data shown is from a solution of 0.3 wt% of 3330 in water with no salt



**Fig. 3** Schematic for dripping-onto-substrate (DoS) rheometry technique (adapted from Dinic et al. (J. Polym. Sci Polym. Phys). The dispensing system comprises of a syringe pump connected to a nozzle. A finite volume of a fluid is pumped through a nozzle on to a substrate. An imaging system consisting of a high-speed camera with attached magnification lenses, a light source, diffuser, and computer is used for capturing the neck shape and neck shape evolution



using the imaging system that consists of a light source with a diffuser and a high-speed camera (Fastcam SA3) with a train of lenses (Nikkor  $\times 3.1$  zoom (18–25 mm) lens, plus a macro lens) attached for obtaining images with high magnification. The radius evolution of the thinning neck is tracked and analyzed with a specially written code in ImageJ and MATLAB to extract radius evolution datasets. For viscoelastic polymer solutions, the neck radius evolution data can be fit to obtain extensional relaxation time and extensional viscosity. At least four measurements were carried out for each composition of the polyelectrolyte solutions.

The interplay of capillary, inertial, viscous, and elastic stresses determine the shape and shape evolution of the fluid neck created in the dripping-onto-substrate set-up as well as for necks formed by stretching liquid bridges or during dripping or jetting (McKinley 2005; Sharma et al. 2015). The characteristic behavior in DoS observed for Newtonian fluids (inviscid as well as viscous), power law fluids, and viscoelastic fluids is detailed elsewhere (Dinic et al. 2017b; McKinley 2005). The inviscid Newtonian fluid response that is exhibited by low viscosity fluids, including water, which is used as the solvent in this study, is associated with the formation of a conical neck. The thinning dynamics of inviscid fluids are described as an inertio-capillary response with a characteristic radius evolution  $R \propto (t_p - t)^{2/3}$ , where  $R$  is the thinnest radius of the neck,  $t$  is time, and  $t_p$  is the critical time for breakup. In contrast, the viscocapillary response shows a linear decrease in radius  $R \propto (t_p - t)$  and is exhibited by the high viscosity Newtonian fluids. Radius evolution follows viscocapillary behavior for Newtonian fluids if the dimensionless viscosity, as characterized by Ohnesorge number,  $Oh = \eta/(\rho\sigma R_0)^{1/2}$  ( $\eta$  is the fluid viscosity,  $\rho$  is the fluid density, and  $\sigma$  is the interfacial or surface tension), is higher than unity (or  $Oh > 1$ ). Addition of polymers dramatically changes the neck radius evolution, often leading

to the emergence of the elastocapillary thinning dynamics that can be described using the following expression based on a theory developed by Entov and Hinch (1997):

$$\frac{R(t)}{R_0} \approx \left( \frac{G_E R_0}{2\sigma} \right)^{\frac{1}{3}} \exp \left[ \frac{-t}{3\lambda_E} \right] \quad (2)$$

Here,  $G_E$  is an apparent extensional modulus,  $\sigma$  is the surface tension, and  $\lambda_E$  represents the extensional relaxation time. The extensional rate,  $\dot{\varepsilon} = -2\dot{R}(t)/R(t)$ , where  $R(t)$  represents the radius at time  $t$ , attains a nearly constant value during the elastocapillary regime, but the extensional strain progressively increases. In some cases, the radius evolution shows a third regime called the finite extensibility regime. The radius evolution in the finite extensibility regime shows a viscocapillary thinning response; however, the effective viscosity is much higher than the solution or solvent viscosity.

For the data analysis presented here, the interfacial tension of all solutions with air is assumed to be 62 mN/m. Several previous studies (Taylor et al. 2007; Okubo 1988) determined that highly charged polymer solutions do not display any dynamic adsorption. However, pendant drop tensiometry measurements carried out for aqueous solutions of lower molecular weight PAA (450 kg/mol) (that were utilized in a parallel rheometry study by Jimenez et al. 2018), interfacial tension decreases to values  $> 62$  mN/m over the course of an hour or more. Thus, for all practical purposes, the dynamic adsorption effects are unlikely to influence both the neck thinning dynamics and the measured values of extensional relaxation time as filament thinning leading to pinch-off occurs in less a second. The absolute value of surface tension affects the computed value of the transient extensional viscosity, but the effect is relatively marginal. The interfacial tension for salt solutions are assumed to be that of the salt solution with no polymer added, (Dutcher et al. 2010) as shown in the Supplementary Information. The extensional viscosity  $\eta_E$  value is extracted

from the ratio of capillary stress  $\sigma/R(t)$  and the extensional rate  $\dot{\epsilon} = -2\dot{R}(t)/R(t)$ , which are both determined from the radius evolution data. Following the procedure outlined by Anna and McKinley, and others (Anna et al. 2001; Miller et al. 2009), the elasto-capillary and finite extensibility regimes were both fit using the following empirical equation:

$$\frac{R(t)}{R_0} = Ae^{-Bt} - Ct + D \tag{3}$$

Here  $A$  is related to the pre-factor in Equation (2),  $B = 1/3\lambda_E$  is inversely proportional to the longest extensional relaxation time, and  $C$  correlates with the steady, terminal extensional viscosity values measured in the finite extensibility regime.

## Results

### Shear rheometry

Typical results comparing the shear ramps and steady shear measurements are shown in Fig. 4. For polyelectrolyte solutions without salt, the shear rate ramps and steady shear data are similar, and show a rate-dependent response. However, upon the addition of salt, higher effective viscosity is observed for the steady shear measurements at relatively low shear rates ( $< 10 \text{ s}^{-1}$ ), and this is accompanied by increased standard deviations at these low shear rates which is also seen in Figs. 5,

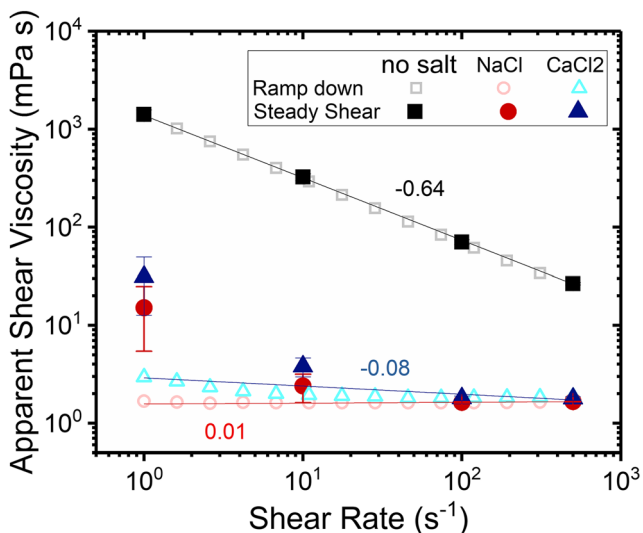


**Fig. 4** Comparison of steady shear data to shear ramps for polyelectrolyte solutions. Data shown from solutions of 0.3 wt% of 3330 in water with no added salt (squares), 0.435 M NaCl (circles), and 0.435 M CaCl<sub>2</sub> (triangles). All steady shear data (filled points) represent ensemble averages and the associated error bars represent one standard deviation of the combined viscosity values for all aliquots from the last 200 s of measurement. Ramp down data (open points) are from a representative single aliquot. Solid lines represent the lines of best fit of the steady shear data; nearby numbers indicate the corresponding slopes

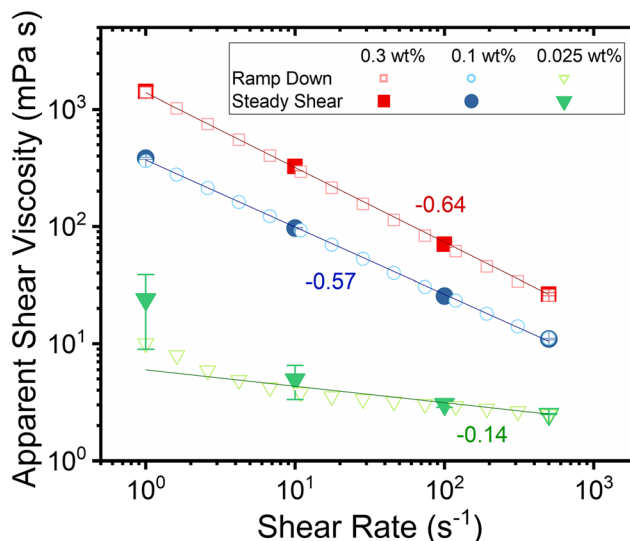


**Fig. 5** Effect of polymer concentration on the shear viscosity of aqueous polyelectrolyte solutions. All data is from aqueous solutions of 0.3 wt% (squares), 0.1 wt% (circles), and 0.025 wt% (triangles) of 3330 with no salt. All steady shear data (filled points) represent ensemble averages; error bars represent one standard deviation of the combined viscosity values for all aliquots from the last 200 s of measurement. Note that ramp down data (open points) are from a representative single aliquot. Solid lines indicate the lines of best fit for the steady shear data; nearby numbers indicate the corresponding slope

6, and 7. Such hysteresis and relatively mild shear thinning response (power law index  $< 0.3$ ) implies that HPAM may form aggregates in aqueous solution and that the deformation of aqueous salt solutions at high shear rates can disrupt these aggregates (Arnolds et al. 2010; Tam et al. 1998).

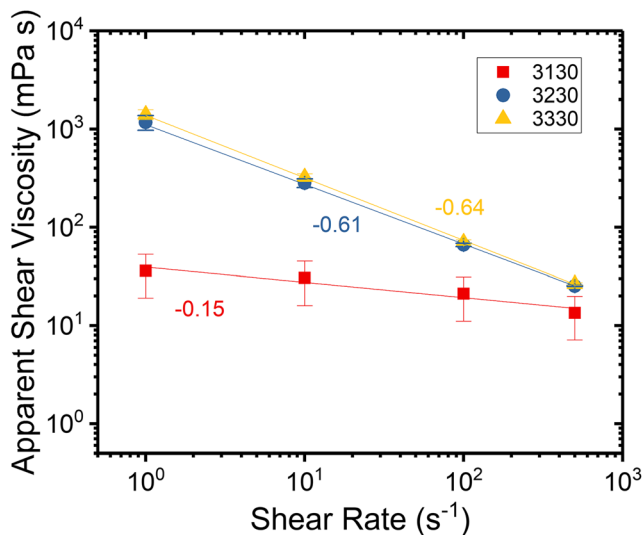


**Fig. 6** Effect of polymer molecular weight on the shear viscosity of polyelectrolyte solutions. All data is from aqueous solutions containing 0.3 wt% of polymer: squares (3130), circles (3230), triangle (3330); all solutions contain no added salt. All points represent ensemble averages; error bars represent one standard deviation of the combined viscosity values for all aliquots from the last 200 s of measurement. Solid lines represent lines of best fit; numbers indicate corresponding slopes

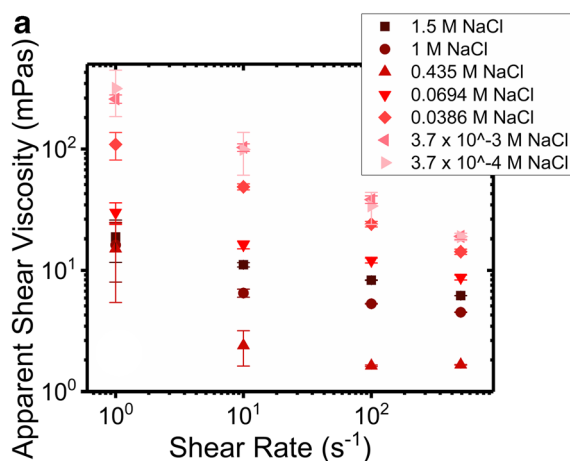
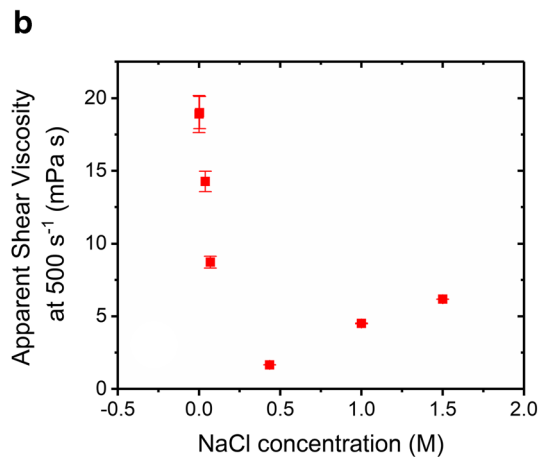


**Fig. 7** Effect of monovalent salt concentration on shear viscosity of aqueous polyelectrolyte solutions. (a) Data is from solutions containing 0.3 wt% of 3330 and  $3.7 \times 10^{-4}$  (light) to 1.5 M NaCl (dark). (b) Shows the data from (a) at  $500 \text{ s}^{-1}$  as a function of monovalent salt concentration.

Indeed, all the aqueous polyelectrolyte solutions investigated show a concentration-dependent increase in steady shear viscosity, as shown in Figs. 5 and 6. The aqueous HPAM solutions display an apparent shear thinning behavior for the range of shear rates investigated, and the magnitude of the apparent shear viscosity agrees with the measurements reported elsewhere (Clarke et al. 2015; Huh et al. 2009; Jung et al. 2013; Sedaghat et al. 2013; Sheng 2011; Veerabhadrapa et al. 2013). For the lowest concentration included in Fig. 5, a rate-independent response is measured at higher shear rates ( $> 100 \text{ s}^{-1}$ ), which is again correlated with the disruption of aggregates at higher deformation rates.

The steady shear viscosity as a function of shear rate shows dramatic shear thinning in Fig. 5 as well as Fig. 6. The measured shear viscosity decreases with decrease in molecular weight. Polymers with lower reported molecular weight show a lower shear viscosity at all shear rates investigated here. The polymers 3330 and 3230 display similar power law behavior ( $n = 0.362$  and  $n = 0.391$ , respectively). On the other hand, 3130 displays a higher power law exponent ( $n = 0.844$ ).

Upon the addition of monovalent salt to polymer solutions, the magnitude of steady shear viscosity decreases at the shear rates investigated as shown in Fig. 7. The steady shear viscosity shows a pronounced shear thinning response for low salt concentrations ( $c_s < 0.435 \text{ M NaCl}$ ) in the shear rate range shown in Fig. 7. However, at  $c_s > 0.435 \text{ M NaCl}$ , the solutions show rate-independent viscosity at higher shear rates ( $\geq 100 \text{ s}^{-1}$ ), while at lower shear rates ( $\leq 10 \text{ s}^{-1}$ ) the solutions exhibit shear thinning response. Fig. 7b also shows a comparison of the shear viscosity values obtained at a nominally high shear rate of  $500 \text{ s}^{-1}$ ; the comparison illustrates the apparent non-monotonic concentration-dependent shear viscosity values for polyelectrolyte solutions at shear rates solutions may encounter in EOR applications. The high shear rate viscosity values



All points represent ensemble averages; error bars represent one standard deviation of the combined viscosity values for all aliquots from the last 200 s of measurement

decrease with added salt up to a concentration of approximately  $0.5 \text{ M NaCl}$ , beyond which the values increase again.

The effect of divalent cations on the steady shear viscosity behavior as a function of shear rate is shown in Fig. 8a, and the absolute value of shear viscosity is compared to that of monovalent salt in Fig. 8b. The presence of  $\text{CaCl}_2$  led to a significant decrease in the rate-dependent viscosity in comparison to both salt-free solutions and the solutions with the same molar concentration of  $\text{NaCl}$ . This can be attributed to more effective screening caused by the higher charge of calcium ions, as well as the possibility of a higher degree of intra- and inter-chain association. The steady shear viscosity behavior shows a rate-independent behavior at high shear rates even though shear thinning response is observed at low shear rate values for solutions with a  $\text{CaCl}_2$  concentration above  $0.0694 \text{ M}$ . Similar behavior is observed for the  $\text{NaCl}$  solutions above a higher critical salt concentration ( $0.435 \text{ M}$ ). While other studies reported precipitation upon the addition of divalent salts (Huh et al. 2009; Rashidi et al. 2010), neither precipitation nor coacervation was observed for the solutions studied here, even after days without agitation. When considering the behavior of solutions as a function of salt concentration, an increase in effective viscosity at the highest divalent salt concentrations is observed. For both  $\text{NaCl}$  and  $\text{CaCl}_2$ , shear viscosity values measured at nominal high shear rate of  $500 \text{ s}^{-1}$  show non-monotonic dependence on the ionic strength of the solutions, as shown in Fig. 8b.

## Extensional rheometry

DoS rheometry relies on visualization and analysis of neck thinning dynamics, and the sequence of images included Fig. 9a–d show the typical neck shapes observed for the HPAM solutions. The radius evolution data is plotted in Fig.

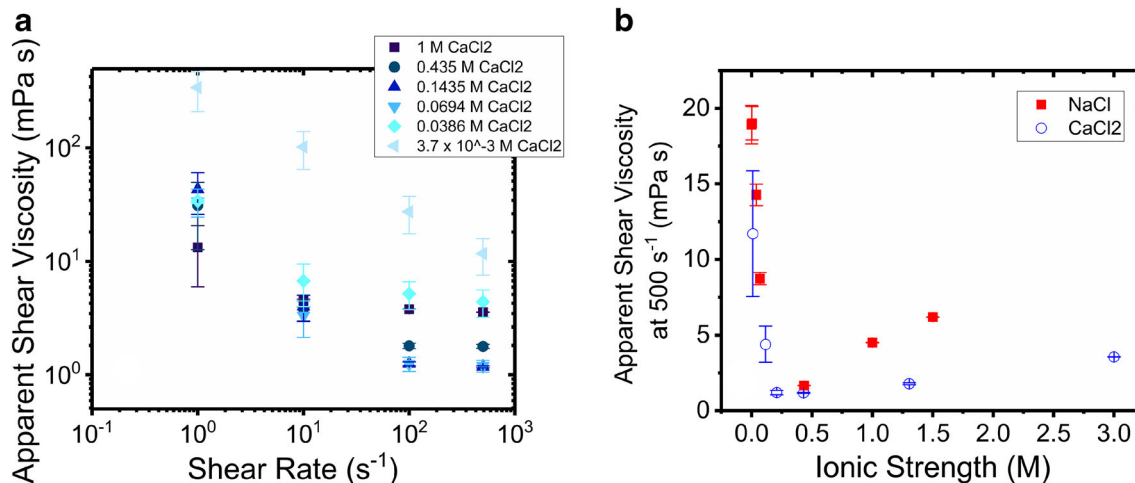


**Fig. 8** Effect of divalent salt concentration on shear viscosity of aqueous polyelectrolyte solutions. (a) Data are from solutions containing 0.3 wt% of 3330 and  $3.7 \times 10^{-3}$  (light) to 1 M CaCl<sub>2</sub> (dark). (b) Comparison of shear viscosity as a function of concentration of NaCl (filled squares) and

CaCl<sub>2</sub> (open circles). All points represent ensemble averages; error bars represent one standard deviation of the combined viscosity values for all aliquots from the last 200 s of measurement

9e and shows three distinct regimes: a sharp transition point separates the inertio-capillary regime from the elastocapillary regime. On a semi-log plot, the radius evolution in the elastocapillary regime appears as linear, and an additional last regime, known as the finite extensibility regime, can be observed in several cases.

The effect of polymer molecular weight and concentration on the extensional relaxation time extracted from the elastocapillary regime in radius evolution data is shown in Fig. 10. Increase in polymer concentration leads to longer relaxation times for the three polymer molecular weights

considered, and the extensional relaxation time increases with molecular weight. The extensional relaxation times measured here are 1–30 ms, and as these values are quite short, such measurements are not possible on CaBER, the commercially-available extensional rheometer that requires more than 50 ms to set-up the liquid bridge (Dinic et al. 2015; Rodd et al. 2005).

As briefly discussed in the methods section, the value of extensional viscosity is calculated from the ratio of capillary stress to the extensional rate. Capillary stress is calculated as  $\sigma/R(t)$  where  $\sigma$  is the surface tension and  $R$  is the neck radius. The extensional rate,  $\dot{\epsilon}$ , is computed using  $\dot{\epsilon} = -2\dot{R}(t)/R(t)$ .

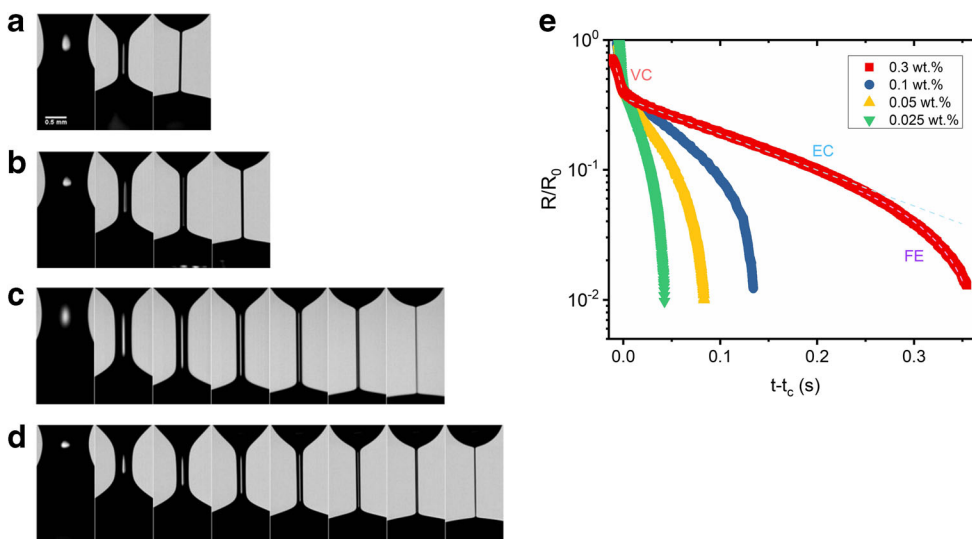


**Fig. 9** Radius evolution over time for aqueous polyelectrolyte solutions obtained using DoS rheometry. Image sequences (a)–(c) 25 ms apart show slender, cylindrical neck shapes for solutions of 0.025%, 0.05% and 0.1 wt% of 3330 in water with no salt, respectively, and the image sequence in (d) has time step of 50 ms for a solution of 0.3 wt% of 3330 in

water. (e) Corresponding radius evolution plots show that concentration dependent variation in both shape of the curves and pinch-off time. As the solution viscosity is relatively high, the data shows an initial visco-capillary region, followed by an elastocapillary region (EC) and before pinch-off, the finite extensibility (FE) regime can be observed



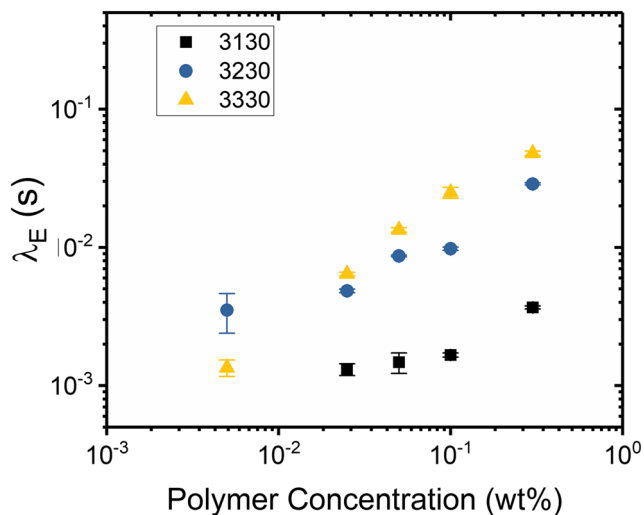


**Fig. 10** Extensional relaxation time as a function of polymer concentration for solutions of FLOPAAM with three different molecular weights water with no salt. Data are extracted from radius evolution data and represent averages; error bars represent one standard deviation. The extensional relaxation time increases with both concentration and molecular weight

Upon careful examination of this method and Equation 2, it becomes clear that increasing extensional relaxation time leads to increasing extensional viscosity and therefore the results in Fig. 10 indicate that the extensional viscosity increases with increasing polymer molecular weight. The concentration-dependent increase in extensional viscosity for polyelectrolyte solutions can be observed in Fig. 11. The elastocapillary regime provides a measurement of the transient extensional viscosity as a function of Hencky strain, whereas the finite extensibility region provides a measure of rate-

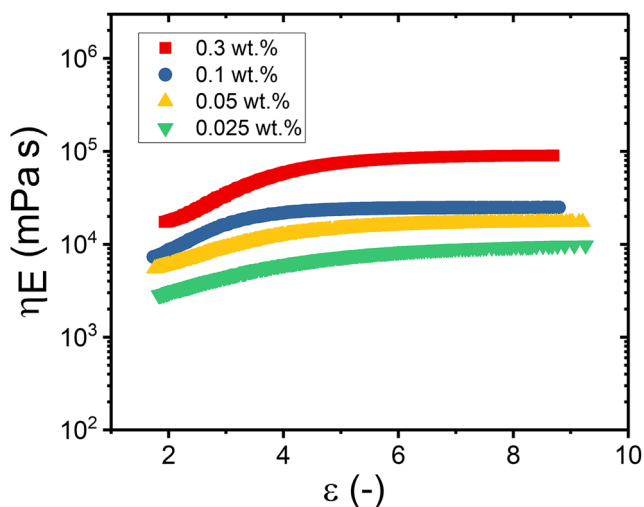


**Fig. 11** Extensional viscosity of polyelectrolyte solutions as a function of Hencky strain. Solutions show strain hardening with increasing polymer concentration. Solutions with higher polymer concentrations have higher extensional viscosities. All data shown is from solutions of 3330 in water with no salt. Curves are from one drop of each solution

independent, strain-independent steady, terminal extensional viscosity. All polyelectrolyte solutions display strain-hardening, or increasing viscosity with increasing extensional strain. The extensional viscosity was found to be several orders of magnitude higher than the shear viscosity and increases with increasing polymer molecular weight. Both transient and steady, terminal extensional viscosity increase with molecular weight and concentration, and display values that are directly proportional to extensional relaxation time, in agreement with literature data (Dinic et al. 2017a; Jimenez et al. 2018).

The presence of either monovalent or divalent salt results in a decrease in both extensional relaxation time and transient extensional viscosity as shown in Fig. 12, and the polyelectrolyte solutions with salt are also strain hardening like their counterparts without salt. Consistent with shear rheometry results, solutions containing higher concentrations of NaCl (1 M) have a lower transient extensional viscosity than solutions with a lower concentration of NaCl (0.0386 M). Further, the solutions containing 1 M of CaCl<sub>2</sub> have longer relaxation times than solutions containing 1 M of NaCl. Of special note are the extremely long strains to which the solution with 1 M CaCl<sub>2</sub> persists in the elasto-capillary regime. The polyelectrolyte solutions in presence of salt are also strain-hardening, quite like the salt-free solutions; however, the terminal extensional viscosity values are lower. The data show that an increase in polymer concentration for a fixed concentration of salt leads to an increase in both extensional relaxation time and extensional viscosity. However, even though the presence of salt ions in the solution decreases the extent of electrostatic stretching leading to a decrease in extensional viscosity, the divalent salt data illustrates the importance of the role played by multivalent ions in promoting formation of stronger interchain interactions.

## Discussion

### Shear rheometry

The weak power law response ( $n < 0.3$ ) displayed by steady shear viscosity as a function of shear rate suggests the presence of aggregates. Though the shear thinning response arises for high molecular weight polymer and polyelectrolyte solutions, typically, the power law index is higher ( $n > 0.6$ ). The very different power law index observed for solutions of 3130 may indicate that there are other additives in the polymer that were not removed, as the polymer was not purified. The onset of shear thinning can be used for defining a shear relaxation time (Colby et al. 2007; Boris and Colby 1998; Colby 2010; Dobrynin et al. 1995; Jimenez et al. 2018), and for semi-dilute polyelectrolyte solutions, as the shear relaxation time decreases with concentration, the critical shear rate at the onset

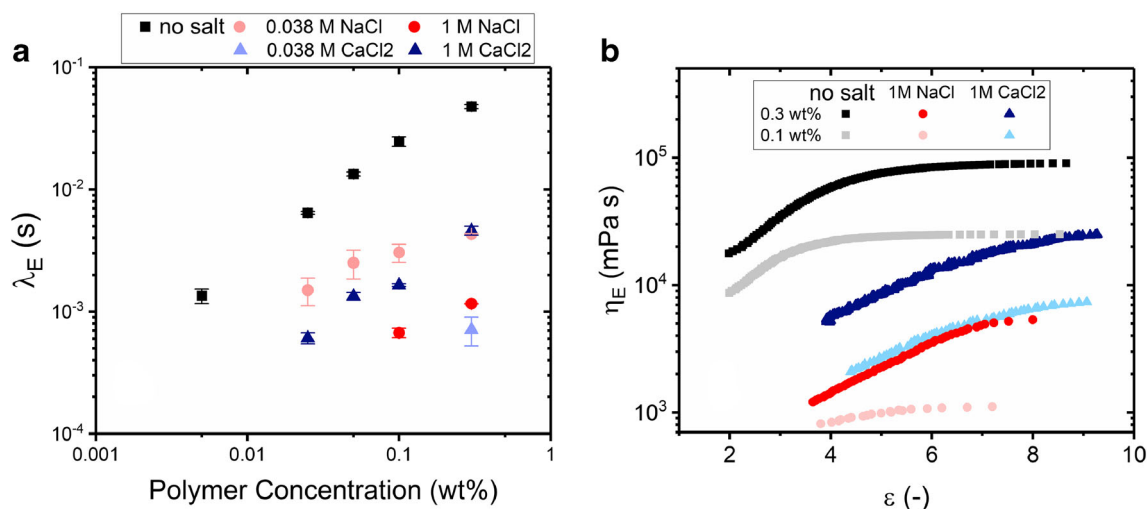


**Fig. 12** Effect of salt and polymer concentration on extensional relaxation time and viscosity. All data shown is from solutions of 3330. Some data not shown because solutions did not display elasto-capillary

of shear thinning regime can increase with concentration. Based on the extensional relaxation time data that shows typical values around 1 ms, the shear thinning regime is not observed for the shear rate range measured.

The change in solution behavior on the addition of salt, shown in Fig. 7, shows trends expected for aqueous polyelectrolyte solutions. Effective shear viscosity is reduced from that in water without salt and shear thinning behavior is maintained, although at high salt concentrations, a Newtonian plateau is observed at high shear rates ( $> 100 \text{ s}^{-1}$ ). The negative charges on the HPAM chains repel each other, causing the polymers to adopt an extended conformation. The increase in the concentration of ions due to the dissolved salt leads to progressive screening of charge. This lowers the repulsion between the charges, lowering the hydrodynamic volume of each polyelectrolyte chain, thus decreasing their degree of overlap and consequently decreasing the viscosity of the solution, consistent with what is observed here.

In this work, the apparent viscosity computed at  $500 \text{ s}^{-1}$  first decreases, then increases with increase in concentration of added monovalent as well as divalent salt as shown in Figs. 7 and 8. Such non-monotonic viscosity variation with monovalent salt concentration could be result of several factors, including the relatively high concentration of polyelectrolyte used (for in entangled regime, high salt leads to increase in solution viscosity), and the possibility of extra interchain interactions including hydrogen bonding promoted by the high degree of screening at high salt concentration (Rashidi et al. 2010; Wyatt et al. 2011; Wyatt and Liberatore 2010). At higher divalent salt concentrations, the divalent cations may complex to the negative charges on the polyelectrolyte chain (Chremos and Douglas 2016), potentially forming ionic bridges that can act as transient crosslinks between charges on two different

behavior. Points in (a) are averages of data from multiple drops; curves in (b) are data from a single representative drop

polyelectrolyte chains (intermolecular complexation) or within the same chain (intramolecular complexation).

Whether the calcium ions complex intermolecularly or intramolecularly may depend on the molecular weight and percent hydrolysis of the HPAM as well as the concentration of calcium in solution (Francois et al. 1997; Huber 1993; Peng and Wu 1999; Schweins and Huber 2001; Ward and Martin 1981). The non-monotonic behavior may be due to a transition between intramolecular bridges at low calcium concentration and intermolecular bridges at high calcium concentration. Additionally, the chloride ions also contribute to screening. Since calcium chloride has twice as much chloride on a molar basis than sodium chloride, the screening effect of the chlorides alone is much greater for solutions with CaCl<sub>2</sub> than NaCl. This higher amount of screening would promote closer polymer-polymer interactions, which may also lead to increased viscosity at high added salt concentration (as described above).

Additionally, the trends illuminated here may be generally applicable to other monovalent and divalent salts; however, variations are expected for different monovalent and divalent salts. Specifically, ion size and hydrated ion radius will have a large impact on the results. As detailed in Wyatt and Liberatore 2010, in solutions of different salts, the replacement of counterions by a counterion of a different size may occur. In highly concentrated polymer solutions in which the polymer chains are close to one another due to the increased screening of the chains caused by the high salt concentration, this change in counterion size could have a noticeable effect. For example, should the introduced counterions from the salt solution be larger than the previous counterions (in the case of poly(acrylic acid) and not poly(sodium acrylate) this would be the case universally), the added volume may force the polymer coils to expand.

## Extensional rheometry

The increase in the value of extensional relaxation times with increase in polymer concentration in salt-free solutions, shown in Fig. 10, is consistent with the shear data reported here and with similar extensional data reported recently by Jimenez et al. (2018) for polyelectrolyte solutions made with both poly(acrylic acid) and sodium poly(styrene sulfonate). The transient extensional viscosity plots as a function of extensional strain show a pronounced strain-hardening. It is well established that polymer coils are only weakly perturbed in shear flow, whereas stretching and orientation in response to high extensional rates can lead to a coil–stretch transition, and even full unraveling of chains in the finite extensibility limit.

In the semi-dilute regime, the shear relaxation time decreases with concentration for unentangled polyelectrolytes, but increases with concentration in the entangled regime. The corresponding scaling law that describes the concentration-dependent shear relaxation time (extracted from shear rheology measurements) is correlated with the concentration-dependent behavior of the correlation blobs. In the case of neutral polymers, chains stretched by hydrodynamics in the semi-dilute regime show a stronger concentration dependent increase in extensional relaxation time, as stretching increases the degree of overlap, as well as screening of excluded volume and hydrodynamic interactions (Dinic et al. 2017a).

The extensional rates generated with the thinning necks are relatively high ( $> 10^3 \text{ s}^{-1}$ ). Therefore, the polymers studied here may stretch during extension, disrupting the hydrogen bonds between polymer chains that cause the increase in shear viscosity shown in Fig. 7. Additionally, this stretch would disrupt any inter- or intramolecular coordination by calcium ions. The increase in extensional relaxation time at higher calcium concentration, shown in Fig. 12a, is approximately one order of magnitude. Compared to the increase in shear viscosity at higher calcium concentrations shown in Fig. 8b, which is within one order of magnitude, this increase during extension suggests that there is a mechanism opposing the stretch of the polymers that is not present (or weak) when shear forces are applied. Taking these differences into consideration, we suggest that the calcium ions in solution are replacing some of the sodium ions as counterions on the polyelectrolyte and that these calcium ions are coordinating negative charges along the polymer chain to each other, either within the same chain or between different chains.

## Application to enhanced oil recovery

The results support the widespread use of HPAM in EOR. The shear thinning nature of the solutions is beneficial during pumping and transportation of the solutions.

Simultaneously, in the extensional flow fields encountered in porous media, the strain hardening behavior of the solutions would promote higher oil recovery by increasing the capillary number and dislodging more trapped oil droplets out of pores. In the past, it has been an open question if the apparent benefits of utilizing HPAM in EOR are negated by the presence of salt or hard water (high calcium concentration). The results in this study show that the addition of salt, either monovalent or divalent, leads to a reduction in both shear and extensional viscosity. Despite this reduction, the shear thinning and strain-hardening behavior remains in the presence of salt, even calcium, ions. Therefore, it is believed that even in high salinity and high hardness, solutions of HPAM would maintain the properties that are beneficial to EOR: shear thinning and strain-hardening.

## Conclusions

The behavior of polyelectrolytes in aqueous solutions with and without added salt has been investigated through shear and extensional rheology. It has been shown that while monovalent and divalent salts both decrease the shear and extensional viscosities of solutions from those without added salts, the effect of the concentration of salt differs between monovalent and divalent salts. The trend with monovalent salts is consistent with previously reported data; higher concentrations of monovalent salt screen negative charges on the polyelectrolyte backbone more effectively. Divalent cations may form transient complexes with the polyelectrolyte chain, causing higher extensional viscosity at high divalent salt concentrations. These features make these solutions attractive for enhanced oil recovery, both when considering fluid transport and behavior in the oil basin. In addition to the application to EOR, this study furthers the understanding of polyelectrolyte-ion interactions that may be applied to a wide variety of functions.

**Funding information** A.V.W. and K.A.E. would like to thank the Pioneer Oil Company (Lawrenceville, Illinois) for providing the FLOPAAM samples and the Purdue Gas and Oil Boiler Innovation Group (GO BIG) for initial project funding. Acknowledgement (K.A.E.) is also made to the Donors of the American Chemical Society Petroleum Research Fund for partial support of this research. V.S. would like to acknowledge funding support by the College of Engineering and the Department of Chemical Engineering at the University of Illinois at Chicago. The students (J.D. & L.N.J.) were supported by the start-up funds as well as funding by the Campus Research Board (CRB). L.N.J. also wishes to acknowledge sustained funding (Teaching Assistantship) by the Department of Chemistry at UIC.

**Publisher's note** Springer Nature remains neutral with regard to jurisdictional claims in published maps and institutional affiliations.

## References

- Advanced Resources International. (2006) Undeveloped domestic oil resources: the foundation for increasing oil production and a viable domestic oil industry. Retrieved from [http://www.tenaskatrailblazer.com/pdfs/library/Undeveloped\\_Oil\\_Resources.pdf](http://www.tenaskatrailblazer.com/pdfs/library/Undeveloped_Oil_Resources.pdf)
- Anna SL, McKinley GH, Nguyen DA, Sridhar T, Muller SJ, Huang J, James DF (2001) An interlaboratory comparison of measurements from filament-stretching rheometers using common test fluids. *J Rheol* 45(1):83–114. <https://doi.org/10.1122/1.1332388>
- Arnolds O, Buggisch H, Sachsenheimer D, Willenbacher N (2010) Capillary breakup extensional rheometry (CaBER) on semi-dilute and concentrated polyethyleneoxide (PEO) solutions. *Rheol Acta* 49(11):1207–1217. <https://doi.org/10.1007/s00397-010-0500-7>
- Boris DC, Colby RH (1998) Rheology of sulfonated polystyrene solutions. *Macromolecules* 31(17):5746–5755. <https://doi.org/10.1021/ma971884i>
- BP (2014) Statistical Review of World Energy June 2014.
- Calvert P (2001) Inkjet printing for materials and devices. *Chem Mater* 13(10):3299–3305
- Chremos A, Douglas JF (2016) Influence of higher valent ions on flexible polyelectrolyte stiffness and counter-ion distribution. *J Chem Phys* 144(16):1–9. <https://doi.org/10.1063/1.4947221>
- Clarke A, Howe AM, Mitchell J, Stanilan J, Hawkes L, Leeper K (2015) Mechanism of anomalously increased oil displacement with aqueous viscoelastic polymer solutions. *Soft Matter* 11:3536–3541. <https://doi.org/10.1039/C5SM00064E>
- Colby RH (2010) Structure and linear viscoelasticity of flexible polymer solutions: comparison of polyelectrolyte and neutral polymer solutions. *Rheol Acta* 49(5):425–442. <https://doi.org/10.1007/s00397-009-0413-5>
- Colby RH, Boris DC, Krause WE, Dou S (2007) Shear thinning of unentangled flexible polymer liquids. *Rheol Acta* 46(5):569–575. <https://doi.org/10.1007/s00397-006-0142-y>
- De Gennes PG, Pincus P, Velasco RM, Brochard F (1976) Remarks on polyelectrolyte conformation. *J de Physique* 37(12):1461–1473
- Dinic J, Zhang Y, Jimenez LN, Sharma V (2015) Extensional relaxation times of dilute, aqueous polymer solutions. *ACS Macro Lett* 4:804–808. <https://doi.org/10.1021/acsmacrolett.5b00393>
- Dinic J, Biagioli M, Sharma V (2017a) Pinch-off dynamics and extensional relaxation times of intrinsically semi-dilute polymer solutions characterized by dripping-onto-substrate rheometry. *J Poly Sci B: Poly Phys* 55(22):1692–1704. <https://doi.org/10.1002/polb.24388>
- Dinic J, Jimenez LN, Sharma V (2017b) Pinch-off dynamics and dripping-onto-substrate (DoS) rheometry of complex fluids. *Lab Chip* 17(3):460–473. <https://doi.org/10.1039/C6LC01155A>
- Dobrynin AV, Colby RH, Rubinstein M (1995) Scaling theory of polyelectrolyte solutions. *Macromolecules* 28(6):1859–1871. <https://doi.org/10.1021/ma00110a021>
- Dunlap PN, Wang CH, Leal LG (1987) An experimental study of dilute polyelectrolyte solutions in strong flows. *J Poly Sci B: Poly Phys* 25(11):2211–2238. <https://doi.org/10.1002/polb.1987.090251101>
- Dutcher CS, Wexler AS, Clegg SL (2010) Surface tensions of inorganic multicomponent aqueous electrolyte solutions and melts. *J Phys Chem A* 114(46):12216–12230. <https://doi.org/10.1021/jp105191z>
- Entov VM, Hinch EJ (1997) Effect of a spectrum of relaxation times on the capillary thinning of a filament of elastic liquid. *J Non-Newtonian Fluid Mech* 72(1):31–53. [https://doi.org/10.1016/S0377-0257\(97\)00022-0](https://doi.org/10.1016/S0377-0257(97)00022-0)
- Francois J, Truong ND, Medjahdi G, Mestdaght MM (1997) Aqueous solutions of acrylamide-acrylic acid copolymers: stability in the presence alkalino earth cations. *Polymer* 38(25):6115–6127. [https://doi.org/10.1016/S0032-3861\(97\)00165-1](https://doi.org/10.1016/S0032-3861(97)00165-1)
- Huber K (1993) Calcium-induced shrinking of polyacrylate chains in aqueous-solution. *J Physical Chem* 97(38):9825–9830. <https://doi.org/10.1021/j100140a046>
- Huh C, Bryant S, Sharma M, Choi SK (2009) pH sensitive polymers for novel conformance control and polymerflood applications. Proc of SPE Intl Symposium on Oilfield Chemistry (December). <https://doi.org/10.2118/121686-MS>
- Jimenez LN, Dinic J, Parsi N, Sharma V (2018) Extensional relaxation time, pinch-off dynamics, and printability of semidilute polyelectrolyte solutions. *Macromolecules*, acs.macromol:8b00148. <https://doi.org/10.1021/acs.macromol.8b00148>
- Jung JC, Zhang K, Chon BH, Choi HJ (2013) Rheology and polymer flooding characteristics of partially hydrolyzed polyacrylamide for enhanced heavy oil recovery. *J Appl Poly Sci* 127(6):4833–4839. <https://doi.org/10.1002/app.38070>
- Katchalsky A, Spitnik P (1947) Potentiometric titrations of polymethacrylic acid. *J Polym Sci* 2(4):432–446. <https://doi.org/10.1002/pol.1947.120020409>
- Lewandowska K (2006) Comparative studies of rheological properties of polyacrylamide and partially hydrolyzed polyacrylamide solutions. *J Appl Phys* 103:2235–2241. <https://doi.org/10.1002/app>
- McKinley GH (2005) Visco-elasto-capillary thinning and break-up of complex fluids. *Polymer* 2005(5):1274–1277. <https://doi.org/10.1007/s00247-009-1482-4>
- Metaxas A, Raethke E, Wilkinson H, Dutcher CS (2018) In situ polymer flocculation and growth in Taylor-Couette flows. *Soft Matter* In press <https://doi.org/10.1039/C8SM01694A>
- Miles MJ, Tanaka K, Keller A (1983) The behaviour of polyelectrolyte solutions in elongational flow: the determination of conformational relaxation times (with an appendix of an anomalous adsorption effect). *Polymer* 24(9):1081–1088. [https://doi.org/10.1016/0032-3861\(83\)90240-9](https://doi.org/10.1016/0032-3861(83)90240-9)
- Miller E, Clasen C, Rothstein JP (2009) The effect of step-stretch parameters on capillary breakup extensional rheology (CaBER) measurements. *Rheol Acta* 48(6):625–639. <https://doi.org/10.1007/s00397-009-0357-9>
- Muggeridge A, Cockin A, Webb K, Frampton H, Collins I, Moulds T, Salino P (2014) Recovery rates, enhanced oil recovery and technological limits. *Philosophical Trans A* 372: 20120320. doi: <https://doi.org/10.1098/rsta.2012.0320>
- Murray LM, Erk KA (2014) Jamming rheology of model cementitious suspensions composed of comb-polymer stabilized magnesium oxide particles. *J Appl Poly Sci* 131:40429. doi: <https://doi.org/10.1002/app.40429>
- Odell JA, Haward SJ (2008) Viscosity enhancement in the flow of hydrolysed poly(acrylamide) saline solutions around spheres: implications for enhanced oil recovery. *Rheol Acta* 47(2):129–137. <https://doi.org/10.1007/s00397-007-0220-9>
- Okubo T (1988) Surface tension of synthetic polyelectrolyte solutions at the air-water interface. *J Colloid Interface Sci* 125(2):386–398. [https://doi.org/10.1016/0021-9797\(88\)90003-3](https://doi.org/10.1016/0021-9797(88)90003-3)
- Olajire AA (2014) Review of ASP EOR (alkaline surfactant polymer enhanced oil recovery) technology in the petroleum industry: prospects and challenges. *Energy* 77:963–982. <https://doi.org/10.1016/j.energy.2014.09.005>
- Pan C (2005) Determination of connate water salinity from preserved core. In International Symposium of the Society of Core Analysis (pp. 1–13). Toronto, Canada
- Peng S, Wu C (1999) Light scattering study of the formation and structure of partially hydrolyzed poly(acrylamide)/calcium(II) complexes. *Macromolecules* 32:585–589
- Petrov AI, Antipov AA, Sukhorukov GB (2003) Base-acid equilibria in polyelectrolyte systems: from weak polyelectrolytes to interpolyelectrolyte complexes and multilayered polyelectrolyte shells. *Macromolecules* 36(26):10079–10086. <https://doi.org/10.1021/ma034516p>



- Radeva T (2001) Physical chemistry of polyelectrolytes. (T. Radeva, Ed.) (99th ed.). CRC Press
- Rashidi M, Blokhuis AM, Skauge A (2010) Viscosity study of salt tolerant polymers. *J Appl Poly Sci* 117:1551–1557. <https://doi.org/10.1002/app>
- Rodd LE, Scott TP, Cooper-White JJ, McKinley GH (2005) Capillary break-up rheometry of low-viscosity elastic fluids. *Appl Rheol* 15(1):12–27. <https://doi.org/10.3933/ApplRheol-15-12>
- Rodríguez-Rivero C, Hilliou L, Martín del Valle EM, Galán MA (2014) Rheological characterization of commercial highly viscous alginate solutions in shear and extensional flows. *Rheol Acta* 53(7):559–570. <https://doi.org/10.1007/s00397-014-0780-4>
- Rubenstein M, Colby RH (2003) Polymer physics. Oxford University Press, Oxford, UK
- Schweins R, Huber K (2001) Collapse of sodium polyacrylate chains in calcium salt solutions. *Euro Physical J E* 5(1):117–126. <https://doi.org/10.1007/s101890170093>
- Sedaghat MH, Ghazanfari MH, Masihi M, Rashtchian D (2013) Experimental and numerical investigation of polymer flooding in fractured heavy oil five-spot systems. *J Petroleum Sci Eng* 108:370–382. <https://doi.org/10.1016/j.petrol.2013.07.001>
- Seright R, Fan T, Wavrik K, Balaban R (2011) New insights into polymer rheology in porous media. *SPE J* 16(1):1–11. <https://doi.org/10.2118/129200-PA>
- Sharma V, Haward SJ, Serdy J, Keshavarz B, Soderlund A, Threlfall-Holmes P, McKinley GH (2015) The rheology of aqueous solutions of ethyl hydroxy-ethyl cellulose (EHEC) and its hydrophobically modified analogue (hmEHEC): extensional flow response in capillary break-up, jetting (ROJER) and in a cross-slot extensional rheometer. *Soft Matter* 11(16):3251–3270. <https://doi.org/10.1039/c4sm01661k>
- Sheng JJ (2011) Polymer flooding. In *Modern chemical enhance oil recovery* (pp. 101–206). doi: <https://doi.org/10.1016/B978-1-85617-745-0.00005-X>
- Shutang G, Huabin L, Hongfu L (1995) Laboratory investigation of combination of alkali/surfactant/polymer technology for Daqing EOR. *SPE Reserv Eng* 10:194–197
- SNF Floerger. FLOPAAM for enhanced oil recovery. Accessed at [http://snf.com.au/downloads/Flopaam\\_EOR\\_E.pdf](http://snf.com.au/downloads/Flopaam_EOR_E.pdf)
- Stoll WM, al Shureqi H, Finol J, Al-Harthy SAA, Oyemade S, de Kruijff A, van Wunnik J, Arkesteijn F, Bouwmeester R, Faber MJ (2011) Alkaline/surfactant/polymer flood: from the laboratory to the field. *SPE Reserv Eng* 14(6):702–712
- Stueber AM, Walter LM (1991) Origin and chemical evolution of formation waters from Silurian-Devonian strata in the Illinois basin, USA. *Geochim Cosmochim Acta* 55(1):309–325. [https://doi.org/10.1016/0016-7037\(91\)90420-A](https://doi.org/10.1016/0016-7037(91)90420-A)
- Stueber AM, Walter LM, Huston TJ, Pushkar P (1993) Formation waters from Mississippian-Pennsylvanian reservoirs, Illinois basin, USA: chemical and isotopic constraints on evolution and migration. *Geochim Cosmochim Acta* 57(4):763–784. [https://doi.org/10.1016/0016-7037\(93\)90167-U](https://doi.org/10.1016/0016-7037(93)90167-U)
- Tam KC, Jenkins RD, Winnik MA, Bassett DR (1998) A structural model of hydrophobically modified urethane - ethoxylate (HEUR) associative polymers in shear flows. *Macromolecules* 31(98):4149–4159. <https://doi.org/10.1021/ma980148r>
- Taylor DJ, Thomas RK, Penfold J (2007) Polymer/surfactant interactions at the air/water interface. *Adv Colloid Interf Sci* 132(2):69–110. <https://doi.org/10.1016/j.cis.2007.01.002>
- Timm BC, Maricelli JJ (1952) Formation waters in Southwest Louisiana. *Bulletin of the American Assoc Petroleum Geologists* 37(2):394–409
- Veerabhadrapa SK, Doda A, Trivedi JJ, Kuru E (2013) On the effect of polymer elasticity on secondary and tertiary oil recovery. *Ind Eng Chem Res* 52(51):18421–18428. <https://doi.org/10.1021/ie4026456>
- Volk N, Vollmer D, Schmidt M, Oppermann W, Huber K (2004) Conformation and phase diagrams of flexible polyelectrolytes. *Adv Poly Sci* 166:29–65. <https://doi.org/10.1007/b11348>
- Ward JS, Martin F (1981) Prediction of viscosity for partially hydrolyzed polyacrylamide solutions in the presence of calcium and magnesium ions. *Soc Petrol Eng J*, 21(October). doi: <https://doi.org/10.2118/8978-PA>
- Weidman JL, Mulvenna RA, Boudouris BW, Phillip WA (2016) Unusually stable hysteresis in the pH-response of poly(acrylic acid) brushes confined within nanoporous block polymer thin films. *J Am Chem Soc* 138(22):7030–7039. <https://doi.org/10.1021/jacs.6b01618>
- Wever DAZ, Picchioni F, Broekhuis AA (2011) Polymers for enhanced oil recovery: a paradigm for structure-property relationship in aqueous solution. *Prog Poly Sci (Oxford)* 36(11):1558–1628. <https://doi.org/10.1016/j.progpolymsci.2011.05.006>
- Wyatt NB, Liberatore MW (2010) The effect of counterion size and valency on the increase in viscosity in polyelectrolyte solutions. *Soft Matter* 6(14):3346–3352. <https://doi.org/10.1039/c000423e>
- Wyatt NB, Gunther CM, Liberatore MW (2011) Increasing viscosity in entangled polyelectrolyte solutions by the addition of salt. *Polymer* 52(11):2437–2444. <https://doi.org/10.1016/j.polymer.2011.03.053>